Earth and Planetary Science Letters 297 (2010) 446–452

Contents lists available at ScienceDirect

Earth and Planetary Science Letters

journal homepage: www.elsevier.com/locate/epsl

Behavior of Mg isotopes during dedolomitization in the Madison Aquifer, South Dakota

Andrew D. Jacobson [a,*], Zhaofeng Zhang [a,b], Craig Lundstrom [b], Fang Huang [b,c]

[a] Department of Earth and Planetary Sciences, Northwestern University, 1850 Campus Dr, Evanston, IL, 60208, USA
[b] Department of Geology, University of Illinois at Urbana-Champaign, Urbana, IL 61801, USA
[c] Institute of Geochemistry and Petrology, ETH Zurich, CH-8092, Zurich, Switzerland

ARTICLE INFO

Article history:
Received 12 January 2010
Received in revised form 14 June 2010
Accepted 22 June 2010

Keywords:
Mg isotopes
groundwater
chemical weathering
fractionation

ABSTRACT

To constrain how Mg isotopes behave during chemical interactions and physical transport in carbonate-rich settings, we measured δ^{26}Mg values of surface water, groundwater, and dolomite samples from the Madison Aquifer, South Dakota. Groundwater in the Madison Aquifer chemically evolves by dedolomitization during transport along a 236 km flow path. Surface streams recharging the aquifer have δ^{26}Mg values of −1.08 and −1.18‰. Following recharge, groundwater δ^{26}Mg values vary between −1.10 and −1.63‰ up to a distance of 20 km. Between 20 and 189 km, δ^{26}Mg values remain nearly constant at −1.40‰, and a final sample at 236 km shows an increase to −1.09‰. Dolomite exhibits a wide range of δ^{26}Mg values between −2.21 and −1.27‰. Reactive-transport modeling and isotope mixing calculations employing previously published major ion mass-balances, ^{87}Sr/^{86}Sr ratios, and δ^{44}Ca values were used to determine whether dedolomitization reactions, namely dolomite dissolution, calcite precipitation, and Mg-for-Na ion-exchange, fractionate Mg isotopes. We tentatively attribute the final δ^{26}Mg value to preferential uptake of ^{24}Mg during Mg-for-Na ion-exchange. Otherwise, we find little evidence of isotopic fractionation and observe instead that δ^{26}Mg conservatively traces lithologic and hydrologic sources. Either isotope exchange between dolomite and water, with a fractionation factor of 0‰, or mixing between different water sources establishes the δ^{26}Mg value of −1.40‰ at 20 km. This value remains unchanged for the next 169 km of water transport because dolomite adds Mg with an average δ^{26}Mg value near −1.40‰, and no other processes cause fractionation. Calcite precipitation is unimportant either because calcite is not a significant sink for Mg or because Mg uptake during calcite precipitation under conditions of chemical equilibrium does not fractionate Mg isotopes. This study suggests Mg isotopes undergo conservative transport in carbonate-rich settings where waters are in chemical equilibrium with respect to major sources and sinks of Mg.

1. Introduction

The cycling of Mg at the Earth's surface is important to several areas in biogeochemistry. For example, magnesium participates in geochemical reactions that control climate (Berner et al., 1983) and the carbonate mineralogy of seawater over geologic timescales (Hardie, 1996). Most studies have used either major ion mass-balances or traditional isotopic proxies, such as ^{87}Sr/^{86}Sr ratios, to indirectly constrain the sources, transport, and fate of Mg (Miller et al., 1993; Negrel et al., 1993). The advent of high-precision methods for measuring Mg isotope ratios (δ^{26}Mg) has provided new opportunities for directly analyzing the Mg cycle (Galy et al., 2001; Young and Galy, 2004; Tipper et al., 2008b; Bolou-Bi et al., 2009; Wombacher et al., 2009). With respect to the terrestrial cycling of Mg, recent studies have suggested that calcite precipitation (Galy et al., 2002; de Villiers et al., 2005; Buhl et al., 2007; Tipper et al., 2008a), silicate weathering (Tipper et al., 2006; Brenot et al., 2008; Pogge von Strandmann et al., 2008), clay mineral formation (Tipper et al., 2006; Brenot et al., 2008; Pogge von Strandmann et al., 2008), and plant uptake (Black et al., 2006; Bolou-Bi et al., 2010) can fractionate Mg isotopes. However, Mg isotope geochemistry has not achieved a predictive capacity compared to other widely utilized isotope tracers, largely because information about the Mg isotope composition of Earth materials is limited, and the magnitude, underlying mechanisms, and even direction of fractionation remain unresolved.

In this study, we examine the downgradient evolution of δ^{26}Mg values along a 236 km flow path in the Madison Aquifer, South Dakota—a confined carbonate aquifer recharging in the igneous Black Hills. The Madison Aquifer is ideally suited for investigating the behavior of Mg isotopes during chemical weathering and subsequent aqueous transport because water–rock interactions have occurred over a much longer timescale (~15 ka) than can be simulated in laboratory experiments, and previous studies have quantified the rates and mass-balances of geochemical reactions controlling bulk Mg

* Corresponding author. Tel.: +1 847 491 3132; fax: +1 847 491 8060.
E-mail address: adj@earth.northwestern.edu (A.D. Jacobson).

0012-821X/$ – see front matter © 2010 Elsevier B.V. All rights reserved.
doi:10.1016/j.epsl.2010.06.038

concentrations along the hydrologic flow path (Plummer et al., 1990; Jacobson and Wasserburg, 2005). We exploit the Madison Aquifer as a natural geochemical reactor and use existing major ion, Sr isotope, and Ca isotope data (Jacobson and Wasserburg, 2005; Jacobson and Holmden, 2008) to constrain the behavior of Mg isotopes.

2. Study site and methods

Detailed descriptions of the study site as well as the samples and their collection method are given in Jacobson and Wasserburg (2005). The Madison Aquifer is the middle of three Paleozoic aquifers in parts of MT, ND, SD, WY, and Canada. The aquifer is composed of Mississippian age Madison Limestone, a grey to buff colored shallow-water marine carbonate containing dolomite (70%), calcite (25%), and anhydrite (4%) with accessory goethite, halite, hematite, quartz, kaolinite, illite, and mixed layer illite–smectite (Thayer, 1983; Busby et al., 1991). Shale and siltstone belonging to the Englewood Formation confine the bottom of the aquifer, while shale and sandstone belonging to the Minnelusa Formation confine the top. The Madison Limestone was locally uplifted and tilted during the Laramide orogeny, which exposed Precambrian basement rocks and Tertiary syenite porphyry intrusions composing the core of the Black Hills. Nearly 70% of the recharge to the aquifer occurs by hydrologic loss as streams originating in gneissic and igneous watersheds cross karstified beds of Madison Limestone draping the flanks of the intrusion (Long and Putnam, 2002). Direct infiltration of precipitation provides the remaining 30% (Long and Putnam, 2002). Following recharge, groundwater flows in a west to east direction with velocities ranging from 2 to 25 m/yr (Downey, 1984; Plummer et al., 1990; Long and Putnam, 2002). Vertical water-mass mixing is negligible (Downey, 1984).

The suite of water samples analyzed in this study consists of two surface water samples (S1 and S2) assumed to represent stream flow recharge waters to the aquifer and eight groundwater samples (W1–W8) assumed to lie along a 236 km hydrologic flow path between the Black Hills and central SD [see Fig. 1a,b in Jacobson and Wasserburg (2005)]. Samples were collected during the summer. S1 was collected from a tributary stream draining the core of the Black Hills, whereas S2 was collected where the tributary intersects outcrop of Madison Limestone. W1–W8 were collected from wells completed in the Madison Aquifer. Groundwater ^{14}C ages range from ~0–30 yrs (W1–W4), ~70 yrs (W5), and ~15,000 yrs (W6–W8) (Plummer et al., 1990). All samples were filtered through acid-cleaned 0.45 μm filters, acidified to pH = 2 with ultrapure HNO_3, and stored in acid-cleaned LDPE bottles prior to analysis.

Four dolomite samples (DOL1, DOL2, DOL3, and DOL4) were collected from outcrop of the Madison Limestone near the location of S2, and one granite sample (GRA1) was collected from outcrop of the Harney Peak Granite a few kilometers to the south of S2 near Mt. Rushmore.

Likewise, two anhydrite samples (ANH1 and ANH2) were taken from Madison Limestone drill core currently stored at the USGS Core Research Center in Denver, CO (Blankennagel et al., 1979). Jacobson and Wasserburg (2005) and Jacobson and Holmden (2008) previously analyzed the major ion, Sr isotope, and Ca isotope composition of DOL1, DOL2, ANH1 and ANH2. Samples DOL3, DOL4 and GRA1 are new samples analyzed for the first time in the present study.

The Mg isotope composition of dolomite was constrained using bulk digestions as well as a two-part sequential leaching and digestion procedure. Bulk digestions were obtained by reacting 0.1 g of powdered dolomite with concentrated HNO_3. Insoluble residues were completely digested using concentrated HF and HNO_3, and the solutions were combined with those from the previous step. In separate experiments, 2 g sub-samples of powdered dolomite were mixed with 20 mL of ultrapure water for 10 h in centrifuge tubes open to atmospheric exchange. Mixtures were centrifuged, and supernatants were passed through 0.45 μm filters, dried, and re-dissolved in concentrated HNO_3. Residues were dried, and 0.1 g sub-samples were reacted with 6 N HCl. Mixtures were centrifuged, and supernatants were passed through 0.45 μm filters, dried, and re-dissolved in concentrated HNO_3. Approximately 0.1°g of powdered granite was completely digested in concentrated HF and HNO_3, and 1 g samples of powdered anhydrite were completely digested in 6 N HCl. Resulting solutions were dried and re-dissolved in 1 N HNO_3. The Mg concentrations of the anhydrite digests were measured using a Varian Vista-MPX ICP-OES at Northwestern University.

All samples were dried in Teflon beakers at 80–90 °C. Residues were treated with concentrated HNO_3 and dried. The previous step was repeated, and the residues were re-dissolved in 1 N HNO_3. Magnesium was separated from matrix elements by loading 0.1 mL of solution (4–50 μg of Mg) onto polyethylene columns containing 0.5 mL of AG-50-X-12 resin (200–400 mesh). Columns were acid cleaned with 6 N HCl and 8 N HNO_3 before loading the resin, and the resin was pre-cleaned multiple times with 8 N HNO_3, ethanol, and 2.8 N HF before storage in 0.5 N HF. In the column, the resin was rinsed with 1 mL of 0.5 N HF and 5 mL of 8 N HNO_3 before being pre-conditioned with 2 mL of 1 N HNO_3. Matrix elements were eluted with 4.5 mL of 1 N HNO_3 before collecting Mg in 7.5 mL of 1 N HNO_3. Aliquots before and after the Mg elution were collected to check yields.

Magnesium isotope ratios were measured with a Nu Plasma MC-ICP-MS at the University of Illinois, Urbana-Champaign. Samples were introduced using a DSN-100 desolvation nebuliser and analyzed with a standard-sample bracketing method. Sample intensities were matched within 10% of the intensity of the standard (DSM-3). The sensitivity was ~80 V/ppm on mass 24 at a typical uptake rate of 100 μL/min. Prior to isotopic analysis, each sample was checked for yield and the concentration of matrix elements (Na, Al, Ca, Mn, Fe and Ni). Yields were greater than 99%. Samples were rejected for analysis if the matrix concentration exceeded 5% of the Mg concentration (see Huang et al., 2009 for a detailed explanation of matrix effects). At least one total procedural blank was analyzed per batch of 20 samples. Blanks were negligible (2 to 15 ng). All $^{26}Mg/^{24}Mg$ and $^{25}Mg/^{24}Mg$ ratios are reported in delta notation relative to DSM-3, where $\delta^{x}Mg = [(^{x}Mg/^{24}Mg)_{sample}/(^{x}Mg/^{24}Mg)_{DSM\text{-}3} - 1] \times 1000$ and x = 25 or 26. Samples were analyzed in replicate (n = 4–5), where uncertainties are reported as two standard deviations of the mean ($2\sigma_{mean}$). Three single element, internal standards were repeatedly measured during the period of analysis. CAM-1 yielded -2.605 ± 0.090‰ ($2\sigma_{mean}$, n = 49), UIMg-1 yielded -1.985 ± 0.151‰ ($2\sigma_{mean}$, n = 30), and FZT-Mg yielded -2.260 ± 0.034‰ ($2\sigma_{mean}$, n = 7). CAM-1 has an accepted $\delta^{26}Mg$ value of −2.60‰ (Galy et al., 2003). Huang et al. (2009) reported a value of -2.00 ± 0.12‰ ($2\sigma_{mean}$, n = 21) for UIMg-1. FZT-Mg has a $\delta^{26}Mg$ value of -2.28 ± 0.03‰ (Fang-Zhen Teng, personal communication). To ensure that matrix effects using the DSN-100 were unimportant and to further test the accuracy of our analytical method, we measured a subset of samples (S1, W1, W5, and W8) as well as the CAM-1 and UIMg-1 standards using a conventional wet plasma technique. No differences were observed.

3. Results

Tables 1 and 2 report $\delta^{26}Mg$ and $\delta^{25}Mg$ values for the rock and water samples, respectively. Table 1 does not include anhydrite because we did not detect Mg in the digestions. When plotted as $\delta^{25}Mg$ versus $\delta^{26}Mg$, all data yield a line with a slope of 0.524 ± 0.014 (2σ) in good agreement with the theoretical equilibrium slope of 0.521 (Young and Galy, 2004). Hereafter, we only discuss $\delta^{26}Mg$.

Harney Peak Granite underlying the recharge zone has a $\delta^{26}Mg$ value of −0.53‰. By comparison, diorite from the Vosges Mountains and paragneiss from the Himalaya Mountains have $\delta^{26}Mg$ values of −0.53 and −0.42‰, respectively (Tipper et al., 2006; Brenot et al.,

Table 1
Mg isotope geochemistry of water samples from the Madison Aquifer.

Sample	Distance (km)	Mg (μmol/L)[a]	$\delta^{26}Mg \pm 2\sigma_{mean}$[b]	$\delta^{25}Mg \pm 2\sigma_{mean}$[b]
S1	0	609	−1.08 ± 0.08	−0.57 ± 0.09
S2	12	950	−1.18 ± 0.13	−0.62 ± 0.07
W1	10	1967	−1.63 ± 0.11	−0.84 ± 0.06
W2	17	1168	−1.10 ± 0.07	−0.55 ± 0.06
W3	20	1074	−1.41 ± 0.09	−0.73 ± 0.07
W4	23	889	−1.40 ± 0.05	−0.71 ± 0.03
W5	38	1251	−1.40 ± 0.08	−0.72 ± 0.05
W6	150	2378	−1.41 ± 0.10	−0.73 ± 0.11
W7	189	2604	−1.42 ± 0.10	−0.75 ± 0.02
W8	236	2197	−1.09 ± 0.08	−0.58 ± 0.05

[a] Data taken from Jacobson and Wasserburg (2005).
[b] n = 4–5.

2008). Bulk Madison Limestone (dolomite) composing the aquifer has δ^{26}Mg values ranging from −1.45 to −1.79‰, with DOL1 similar to DOL3 and DOL2 similar to DOL4. These results are broadly consistent with dolomite analyses reported elsewhere (Galy et al., 2002; Brenot et al., 2008; Tipper et al., 2008a). The bulk rock δ^{26}Mg values are generally indistinguishable from the water and acid leachate values, with the exception of the water leachate for DOL3, which has a more negative δ^{26}Mg value of −2.21‰. All other leachate values range between −1.27 to −1.81‰. The wide range of δ^{26}Mg values makes it difficult to identify a single dolomite weathering end-member. In the model calculations presented below, we consider a range of possible values but ultimately conclude the end-member must be very close to −1.40‰.

Fig. 1 shows δ^{26}Mg values as a function of distance along the flow path. The surface water collected from the core of the Black Hills (S1) has $\delta^{26}Mg = -1.08$‰, and the surface water collected at the hydrologic loss zone (S2) has $\delta^{26}Mg = -1.18$‰. Insufficient information exists to confidently address why the surface streams have different δ^{26}Mg values relative to the granite that they drain. Possible explanations include fractionation during soil formation or the preferential weathering of minerals with low δ^{26}Mg values compared to the bulk rock. Groundwater samples W1 and W2 display δ^{26}Mg values of −1.63 and −1.10‰, respectively. Samples W3–W7, which span 169 km of water transport, all have δ^{26}Mg values near −1.40‰. Sample W8 at the end of the flow path has $\delta^{26}Mg = -1.09$‰.

4. Discussion

Groundwater in the Madison Aquifer chemically evolves by dedolomitization (Plummer and Back, 1980; Back et al., 1983; Plummer et al., 1990; Naus et al., 2001; Jacobson and Wasserburg, 2005). According to this reaction pathway, the irreversible dissolution of anhydrite by water in chemical equilibrium with respect to dolomite and calcite leads to dolomite dissolution and calcite precipitation according to the following generalized reaction:

$$CaSO_4 + CaMg(CO_3)_2 \rightarrow 2CaCO_3 + Mg^{2+} + SO_4^{2-} \quad (1)$$

Dolomite dissolution and calcite precipitation occur during small fluctuations about the state of chemical equilibrium. Accordingly, intrinsic carbonate mineral reaction rates in the Madison Aquifer are orders of magnitude slower than those obtained in laboratory experiments (Jacobson and Wasserburg, 2005). Halite dissolution and Mg-for-Na ion-exchange also occur, but these reactions are negligible between S1 and W7 (0–189 km). All reaction rates greatly increase between W7 and W8 (189–236 km), especially Mg removal by Mg-for-Na ion-exchange. The net effect is that Mg concentrations linearly increase from 609 to 2604 μmol/L between S1 and W7 but then moderately decline to 2197 μmol/L between W7 and W8 (Jacobson and Wasserburg, 2005).

To understand the downgradient δ^{26}Mg trend shown in Fig. 1, we adapt the steady-state 1D reactive-transport model presented in Jacobson and Wasserburg (2005). Consistent with previous studies of the Madison Aquifer, the model implicitly assumes that the composition of recharge waters has not changed appreciably over the time span represented by the samples (Plummer et al., 1990). The equation describing the rate at which the Mg concentration of water (w) changes as a function of distance (dx) along the flow path is:

$$\nu \frac{dMg_w}{dx} = F_{dol} - F_{ixc}, \quad (2)$$

where ν is the water velocity, F_{dol} is the rate at which dolomite dissolution adds Mg, and F_{ixc} is the rate at which Mg-for-Na ion-exchange removes Mg. Similarly, the equation describing how the Mg isotope composition of water ($\delta^{26}Mg_w$) changes with downgradient distance is:

$$Mg_w(x)\nu \frac{d\delta^{26}Mg_w}{dx} = F_{dol}\left(\delta^{26}Mg_{dol} - \delta^{26}Mg_w\right) - F_{ixc}\Delta_{ixc-w}, \quad (3)$$

where $Mg_w(x)$ is the dissolved Mg concentration at position x determined from Eq. (2), $\delta^{26}Mg_{dol}$ is the Mg isotope composition of

Table 2
Mg isotope geochemistry of dolomite (DOL) and granite (GRA) samples from the Madison Aquifer.

Sample	$\delta^{26}Mg \pm 2\sigma_{mean}$[a]	$\delta^{25}Mg \pm 2\sigma_{mean}$[a]
GRA1	−0.53 ± 0.05	−0.27 ± 0.03
DOL1		
Bulk	−1.76 ± 0.08	−0.93 ± 0.10
H_2O leachate	−1.81 ± 0.17	−0.93 ± 0.07
6 N HCl leachate	−1.76 ± 0.12	−0.91 ± 0.07
DOL2		
Bulk	−1.45 ± 0.09	−0.77 ± 0.08
H_2O leachate	−1.32 ± 0.08	−0.70 ± 0.09
6 N HCl leachate	−1.58 ± 0.10	−0.82 ± 0.07
DOL3		
Bulk	−1.79 ± 0.10	−0.94 ± 0.05
H_2O leachate	−2.21 ± 0.17	−1.16 ± 0.15
6 N HCl leachate	−1.87 ± 0.05	−0.97 ± 0.07
DOL4		
Bulk	−1.51 ± 0.16	−0.78 ± 0.12
H_2O leachate	−1.27 ± 0.16	−0.65 ± 0.07
6 N HCl leachate	−1.63 ± 0.05	−0.84 ± 0.06

[a] n = 4–5.

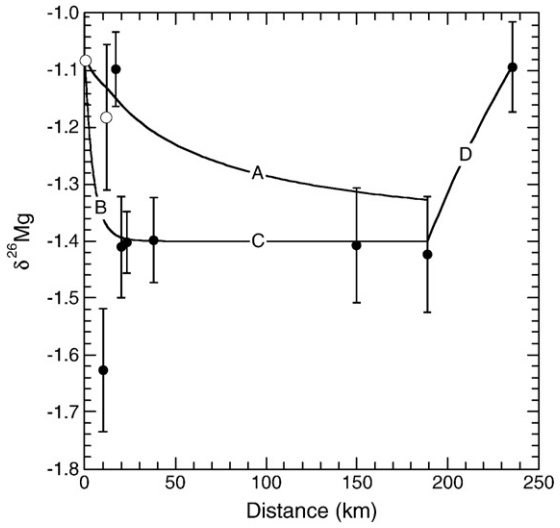

Fig. 1. δ^{26}Mg versus distance (km) for Madison Aquifer surface- and groundwater samples (open and solid circles, respectively). Error bars show $2\sigma_{mean}$ reported in Table 1. Solid curves labeled A, B, C, and D display model output for scenarios described in Sections 4.1, 4.2, 4.4, and 4.5 of text, respectively.

dolomite; $\Delta_{ixc\text{-}w}$ is the approximate isotope fractionation factor associated with Mg-for-Na ion-exchange, and the remainder of the parameters are defined above. Here, $\Delta_{ixc\text{-}w} = \delta^{26}Mg_{ixc} - \delta^{26}Mg_w \approx 10^3 \ln\alpha_{ixc\text{-}w}$, where $\alpha_{ixc\text{-}w}$ is the isotope fractionation factor. In accord with previous studies (e.g., Pogge von Strandmann et al., 2008), we consider that fractionation could discriminate either ^{26}Mg or ^{24}Mg. Hence, $\Delta_{ixc\text{-}w} < 0‰$ means ion-exchange preferentially removes ^{24}Mg over ^{26}Mg, $\Delta_{ixc\text{-}w} = 0‰$ means no fractionation, and $\Delta_{ixc\text{-}w} > 0‰$ means ion-exchange preferentially removes ^{26}Mg over ^{24}Mg. The model only considers fractionation during Mg removal because questions remain whether reported instances of fractionation during Mg addition reflect mass discrimination solely between the dissolving mineral and the surrounding fluid or more likely, the influence of additional processes, such as clay mineral formation and plant uptake (e.g., Brenot et al., 2008; Pogge von Strandmann et al., 2008). These latter processes are not expected for dolomite dissolution in the Madison Aquifer.

We use Eqs. (2) and (3) to constrain processes that could best explain the observed water data. The rate parameters (F values) are given in Table 3. These rates, which were calculated using inverse mass-balances for Cl, Na, Mg, SO_4, and total inorganic carbon (C_T), are "effective", in that they describe the rate at which dissolution and ion-exchange either add or remove Mg to produce the observed water chemistry for a specified value of ν. The rates reported in Table 3 correspond to $\nu = 2$ m/yr (Jacobson and Wasserburg, 2005). As discussed in Jacobson and Wasserburg (2005), two sets of F values exist, one for flow path segment S1–W7 and one for W7–W8. Because the reaction rates are linear, F values for segment S1–W7 also apply to any smaller segment between S1 and W7. The same holds for W7–W8. Segments with the same F values yield the same $\Delta_{ixc\text{-}w}$ values. Lastly, we note the order in which F values are calculated using major ion mass-balances does not permit quantification of the rate at which calcite precipitation might remove Mg from solution. Hence, Eqs. (2) and (3) do not consider Mg isotope fractionation by calcite precipitation. However, as discussed below, it is unlikely that calcite precipitation affects Mg isotope transport in the Madison Aquifer.

4.1. δ^{26}Mg values of groundwater between 0 and 189 km

We first consider the entire flow path segment S1–W7 by setting $\Delta_{ixc\text{-}w} = 0‰$ and $\delta^{26}Mg_{dol} = -1.40‰$. As illustrated by line A in Fig. 1, model $\delta^{26}Mg_w$ values change at a more gradual rate compared to measured values. Between S1 and W3 (0–20 km), model values change from −1.08 to −1.13‰, whereas measured values change from −1.08 to −1.41‰. Reproducing the observed trend requires ion-exchange to preferentially remove ^{26}Mg. However, $\Delta_{ixc\text{-}w}$ is unreasonably high (+45‰) and must switch to 0‰ at W3 (20 km) to maintain $\delta^{26}Mg_w = -1.40‰$ until W7 (189 km). With $\Delta_{ixc\text{-}w} = 0‰$ and $\delta^{26}Mg_w = -1.40‰$ at x = 20 km, the model predicts $\delta^{26}Mg_{dol} = -2.30‰$, which is also consistent with results reported in Table 2. However, to maintain $\delta^{26}Mg_w = -1.40‰$ until W7, ion-exchange must preferentially remove ^{24}Mg with an unreasonably low fractionation factor (−45‰). These effects attributed to $\Delta_{ixc\text{-}w}$ are unlikely. Because surface streams recharging the aquifer (S1 and S2) have relatively low Mg concentrations, model results are insensitive to assumed changes in the isotopic composition of the input waters, such as those resulting from weathering of Harney Peak Granite with a δ^{26}Mg value different than −0.53‰. Below, we consider alternative mechanisms to explain the Mg isotope composition of groundwater during the first 20 km of water transport, namely isotope exchange and water-mass mixing.

Table 3
Reaction rates controlling the input and output of dissolved Mg to Madison Aquifer groundwater[a,b].

Segment	F_{dol}[c]	F_{ixc}[d]
	($\times 10^{-2}$ μmol Mg/L/yr)	
S1–W7[e]	2.12	−0.0420
W7–W8	5.40	−6.75

[a] Calculated according to data presented in Jacobson and Wasserburg (2005).
[b] Negative sign indicates removed from solution.
[c] Rate of Mg addition by dolomite dissolution.
[d] Rate of Mg removal by ion-exchange.
[e] S1–W3 and W3–W7 experience the same reaction rates as S1–W7; see text.

4.2. δ^{26}Mg values of groundwater between 0 and 20 km: isotope exchange

The aquifer waters are in chemical equilibrium with respect to dolomite (Jacobson and Wasserburg, 2005), and dolomite in the Madison Limestone exhibits textural and geochemical evidence for recrystallization (Smith and Dorobek, 1993; Al-aasm, 2000). We thus consider that isotope exchange between dolomite and water could occur when dolomite recrystallizes about the state of chemical equilibrium. Consistent with previous investigations of isotope exchange in water–rock systems (Richter and DePaolo, 1987; Johnson and DePaolo, 1994; Johnson and DePaolo, 1997), we make the following assumptions: Dolomite-water isotope exchange occurs as a normal "slow" reaction that adds Mg with the same isotope composition as that added by dolomite dissolution. The net transfer of Mg atoms is zero such that isotope exchange does not affect groundwater Mg concentrations. Lastly, the transfer of Mg from groundwater to dolomite does not significantly alter the Mg isotope composition of dolomite, which is reasonable given the much higher abundance of Mg in dolomite versus water. With these assumptions, Eq. (2) remains unchanged and Eq. (3) becomes:

$$Mg_w(x)\nu\frac{d\delta^{26}Mg_w}{dx} = F_{dol}\left(\delta^{26}Mg_{dol} - \delta^{26}Mg_w\right) + F'_{dol}\left(\delta^{26}Mg_{dol} - \delta^{26}Mg_w\right) - F'_{dol}\Delta_{dol-w} - F_{ixc}\Delta_{ixc-w}, \quad (4)$$

where F'_{dol} is the rate of Mg exchange between dolomite and groundwater during dolomite recrystallization, and $\Delta_{dol\text{-}w}$ is the fractionation factor for the transfer of Mg from groundwater to dolomite. Following from above, we set $\Delta_{ixc\text{-}w} = 0‰$. We also set $\Delta_{dol\text{-}w} = 0‰$. This implies that dolomite recrystallization does not fractionate Mg isotopes under conditions of chemical equilibrium, which we argue below is reasonable if Mg isotope exchange occurs in the Madison Aquifer. Thus, setting $\delta^{26}Mg_{dol} = -1.40‰$ yields $F'_{dol} = 0.25$ μmol/L/yr, which is over one order of magnitude higher than the rate at which dolomite dissolution irreversibly adds Mg, F_{dol} (see Table 3). As shown by line B in Fig. 1, Eqs. (2) and (4) yield the δ^{26}Mg value expected for W3. The value for F'_{dol} decreases for $\delta^{26}Mg_{dol} < -1.40‰$. However, if $\delta^{26}Mg_{dol} < -1.40‰$, then $\Delta_{dol\text{-}w}$ must become negative at the position of W3 to maintain $\delta^{26}Mg_w = -1.40‰$ until the position of W7. Likewise, if $\delta^{26}Mg_{dol} > -1.40‰$, then $\Delta_{dol\text{-}w}$ must be positive until the position of W3 and then become zero to maintain $\delta^{26}Mg_w = -1.40‰$ until the position of W7. Similar to the problems encountered above with respect to $\Delta_{ixc\text{-}w}$, we think this variability attributed to $\Delta_{dol\text{-}w}$ is unlikely. We thus infer that $F'_{dol} = 0.25$ μmol/L/yr, obtained with the conditions $\Delta_{ixc\text{-}w} = 0‰$, $\Delta_{dol\text{-}w} = 0‰$, and $\delta^{26}Mg_{dol} = -1.40‰$, provides the most plausible result for this scenario. If correct, this finding implies dolomite–water interaction is faster and more dynamic than previously realized. Bulk Mg concentrations only provide insight into the relatively slow rate of dolomite dissolution, whereas δ^{26}Mg values could reveal more rapid exchange of Mg isotopes during dolomite recrystallization.

4.3. δ^{26}Mg values of groundwater between 0 and 20 km: water-mass mixing

Mixing between different recharge waters could also explain groundwater δ^{26}Mg values during the first 20 km of water transport. Hydrologic models have shown that the Madison Aquifer receives ~70% of its recharge from stream flow loss and ~30% from the infiltration of rainfall and snowmelt (Long and Putnam, 2002). We can reasonably assume S1 represents the composition of stream flow recharge, and following discussion in Jacobson and Wasserburg (2005), we note W1 represents the composition of infiltrating precipitation that has interacted with Madison Limestone but not Harney Peak Granite. Figs. 2 and 3 display δ^{26}Mg values for all water samples plotted versus their ^{87}Sr/^{86}Sr ratios and δ^{44}Ca values previously reported in Jacobson and Wasserburg (2005) and Jacobson and Holmden (2008), respectively. Also shown are two-component mixing lines connecting S1 and W1. Dash marks denote the fraction of water originating from S1. The mixing equations implicitly assume bulk solute concentrations and isotopic abundances are conservative. Previous studies of the Madison Aquifer have demonstrated Mg and Sr concentrations are conservative. Calcium is non-conservative due to calcite precipitation. However, the amount of Ca removed over the spatial distance considered is negligible, and calcite precipitation does not fractionate Ca isotopes in the Madison Aquifer (Jacobson and Holmden, 2008). We do not consider effects from evaporation and dilution. Likewise, insufficient information exists to assess seasonal variations in the composition of the end-members.

Figs. 2 and 3 display nearly identical patterns. As expected, S2 plots near the position of S1. W2 also plots near the position of S1 because the well from where this sample was collected receives an unusually high percentage of stream flow recharge (Jacobson and Wasserburg, 2005). Importantly, the next samples along the flow path, W3 (20 km) and W4 (23 km), have δ^{26}Mg values of −1.40‰, consistent with the point where stream flow recharge contributes ~70% of the water to the aquifer. Setting the stream flow end-member equal to S2 instead of S1 yields the same result. Because this finding independently verifies conclusions drawn from hydrologic models of the Madison Aquifer (Long and Putnam, 2002), we conclude that water mixing could also explain the Mg isotope composition of recharge waters, which further implies that Mg isotopes do not fractionate during mixing. In detail however, it is difficult to discern which of the aforementioned scenarios is correct. Magnesium isotope exchange between dolomite and water seems probable, yet such effects were not observed for calcium isotopes (Jacobson and Holmden, 2008). The excellent agreement between isotope mixing equations and hydrologic models is equally compelling, but it seems fortuitous that the byproduct of mixing yields a groundwater δ^{26}Mg value exactly equivalent to the average δ^{26}Mg value identified for dolomite.

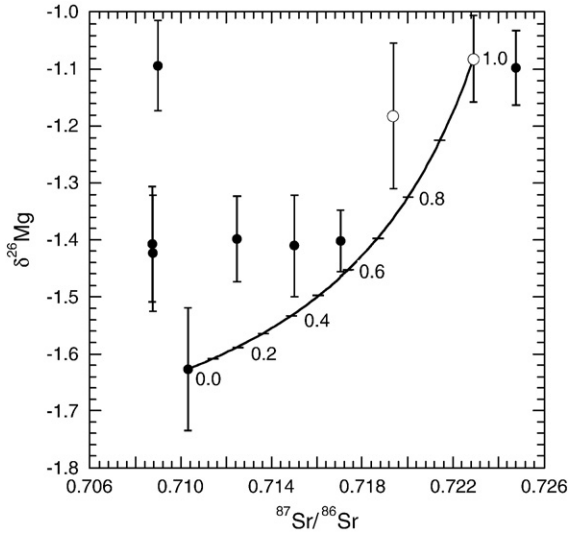

Fig. 2. δ^{26}Mg versus ^{87}Sr/^{86}Sr for Madison Aquifer surface- and groundwater samples (open and solid circles, respectively). Error bars for δ^{26}Mg show $2\sigma_{mean}$ reported in Table 1. Dashed lines show fraction of water originating from stream flow recharge (S1) relative to precipitation infiltration (W1). ^{87}Sr/^{86}Sr ratios taken from Jacobson and Wasserburg (2005).

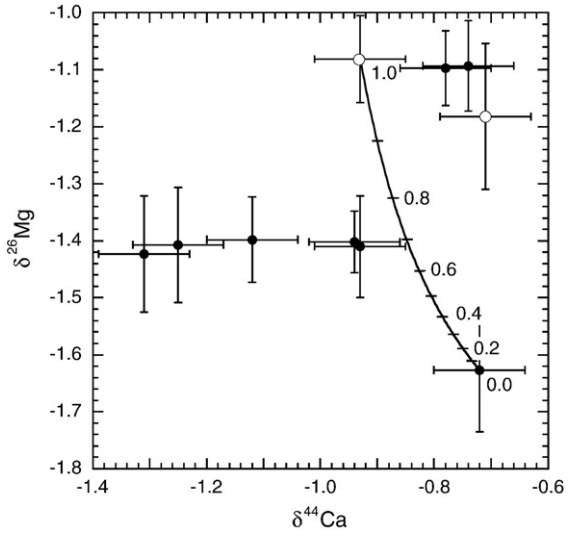

Fig. 3. δ^{26}Mg versus δ^{44}Ca for Madison Aquifer surface- and groundwater samples (open and solid circles, respectively). Error bars for δ^{26}Mg show $2\sigma_{mean}$ reported in Table 1. Error bars for δ^{44}Ca show $2\sigma_{ext} = \pm 0.08$‰. Dashed lines show fraction of water originating from stream flow recharge (S1) relative to precipitation infiltration (W1). δ^{44}Ca values taken from Jacobson and Holmden (2008).

4.4. δ^{26}Mg values of groundwater between 20 and 189 km

Regardless of the mechanism controlling δ^{26}Mg values during groundwater recharge, the δ^{26}Mg value of −1.40‰ established at 20 km remains unchanged for the next 169 km of water transport ($d\delta^{26}Mg_w/dx = 0$) while ^{87}Sr/^{86}Sr ratios and δ^{44}Ca values trend towards the composition of anhydrite (Jacobson and Wasserburg, 2005; Jacobson and Holmden, 2008). Anhydrite dissolution does not influence δ^{26}Mg values because anhydrite does not contain appreciable Mg. Simultaneously, the concentration of dissolved Mg increases from 1074 to 2604 μmol/L (Table 1). Consideration of these observations in the context of Eqs. (2) and (3) implies that $\Delta_{ixc\text{-}w}$ and $\delta^{26}Mg_{dol}$ must be close to 0 and −1.40‰, respectively (line C in Fig. 1). In other words, δ^{26}Mg conservatively traces the progressive addition of dolomite-derived Mg, but an isotopic gradient does not exist because dolomite adds Mg with an isotope composition similar to that of groundwater, and the relatively slow rate of Mg-for-Na ion-exchange does not elicit significant fractionation in this region of the aquifer.

Other more complicated scenarios could explain the lack isotopic variation between W3 and W7, but none seem exceptionally likely. For example, if we set $\delta^{26}Mg_w = -1.40$‰ at x = 20 km as the initial condition for Eq. (3), and we set $\delta^{26}Mg_{dol} = -1.60$‰ (the approximate value for W1), then $\Delta_{ixc\text{-}w}$ must equal −9‰ to maintain $\delta^{26}Mg_w = -1.40$‰ until W7. Similarly, if we set $\delta^{26}Mg_{dol} = -1.30$‰, then $\Delta_{ixc\text{-}w}$ must equal +5‰. These model fractionation factors again exceed the magnitude presently expected for Mg isotopes (Young and Galy, 2004). Even if we assign a hypothetical value of −1.00‰ to $\Delta_{ixc\text{-}w}$, and we set $\delta^{26}Mg_{dol}$ to either −1.60 or −1.30‰, then additional inputs and outputs are required that fortuitously balance the effects of dolomite dissolution and ion-exchange such that $\delta^{26}Mg_w = -1.40$‰ and $d\delta^{26}Mg_w/dx = 0$. The need for isotopic mass balance increases the further $\delta^{26}Mg_{dol}$ deviates from −1.40‰. The observation that $d\delta^{26}Mg_w/dx = 0$ over such a large transport distance

argues against major isotopic effects that would more likely manifest as either $d\delta^{26}Mg_w/dx \neq 0$ or $\delta^{26}Mg_w \neq -1.40‰$ when $d\delta^{26}Mg_w/dx = 0$. Equilibrium isotope exchange between dolomite and water provides a good example. If $\Delta_{dol\text{-}w} \neq 0‰$ and F'_{dol} is relatively low, then $d\delta^{26}Mg_w/dx \neq 0$ would occur, with the exact gradient dependent on the value for $\delta^{26}Mg_{dol}$. If $\Delta_{dol\text{-}w} \neq 0‰$ and F'_{dol} is relatively high, then the condition $\delta^{26}Mg_w \neq -1.40‰$ when $d\delta^{26}Mg_w/dx = 0$ would occur, with the exact value for $\delta^{26}Mg_w$ again dependent on the value for $\delta^{26}Mg_{dol}$. If $\Delta_{dol\text{-}w}$ is nonzero, then $\Delta_{ixc\text{-}w}$ must also be nonzero and of sufficient magnitude to coincidentally yield $\delta^{26}Mg_w = -1.40‰$ and $d\delta^{26}Mg_w/dx = 0$. Given the improbability of these scenarios, we think the simplest explanation above, namely $\Delta_{ixc\text{-}w} = 0‰$ and $\delta^{26}Mg_{dol} = -1.40‰$, is the most reasonable.

4.5. δ^{26}Mg values of groundwater between 189 and 236 km

For segment W7–W8, we set $\delta^{26}Mg_{dol} = -1.40‰$. This leaves fractionation during Mg-for-Na ion-exchange as a potential explanation for the ^{26}Mg enrichment in W8 relative to W7. The model equations yield $\Delta_{ixc\text{-}w} = -0.60‰$, implying ion-exchange preferentially selects ^{24}Mg over ^{26}Mg (line D in Fig. 1). The direction of fractionation is in good qualitative agreement with laboratory studies of Mg isotope adsorption on manganese oxide (Kim et al., 2002), and the magnitude of the fractionation factor appears reasonable for natural systems (Young and Galy, 2004). The effect of ion-exchange is evident for segment S7–S8 because the rate of Mg removal is ~160 times higher compared to the preceding segment. A fractionation factor of −0.60‰ is too small to be resolved for segment S1–S7. Our finding could be the first evidence that ion-exchange fractionates Mg isotopes in nature, which is significant given the widespread occurrence of ion-exchange phenomena. However, with only two samples composing the final segment of the flow path, we caution against invoking ion-exchange as a common fractionation mechanism without further testing.

4.6. Role of calcite precipitation?

Because calcite precipitation is important to the overall dedolomitization reaction pathway, the question arises whether calcite precipitation fractionates Mg isotopes. Speleothem studies suggest calcite precipitation preferentially incorporates ^{24}Mg with a fractionation factor between −2.5 and −2.9‰ (Galy et al., 2002), but it remains unknown whether fractionation represents kinetic processes, equilibrium processes, or some mixture of the two (Buhl et al., 2007). As explained previously, we cannot determine if calcite precipitation influences the dissolved Mg budget of Madison groundwaters. Nonetheless, we can conduct simple thought experiments to constrain possible effects. For the flow path segment between W3 and W7, if we set $\delta^{26}Mg_{dol} = -1.40‰$ and attribute the requisite Mg output to calcite precipitation instead of ion-exchange, then we infer that calcite precipitation does not fractionate Mg isotopes. Similar to above, fractionation factors attributed to calcite precipitation become unreasonably large if we set $\delta^{26}Mg_{dol}$ to either −1.60 or −1.30‰. Likewise, if we attribute a portion of the requisite Mg output to ion-exchange and the remainder to calcite precipitation, then the outputs must either have fractionation factors of 0‰ or fractionation factors with opposite signs and sufficient magnitudes that fortuitously yield $\delta^{26}Mg_w = -1.40‰$ and $d\delta^{26}Mg_w/dx = 0$. Because calcite precipitation appears unimportant for the flow path segment between W3 and W7, we infer the same for the segment between W7 and W8. While these scenarios are very general and require further investigation, they qualitatively suggest calcite precipitation in the Madison Aquifer does not fractionate Mg isotopes. This could arise because calcite precipitation is not a significant sink for Mg in this setting or because uptake of Mg during calcite precipitation under conditions of chemical equilibrium does not fractionate Mg isotopes, similar to the behavior of Ca isotopes (Jacobson and Holmden, 2005). This implies, but does not confirm, that other instances of Mg isotope fractionation by calcite precipitation are kinetically controlled (Galy et al., 2002; de Villiers et al., 2005; Buhl et al., 2007; Tipper et al., 2008a).

5. Conclusions and implications

Magnesium isotopes experience negligible fractionation during physical transport and chemical interactions throughout most of the Madison Aquifer. This behavior is identical to that previously observed for Ca isotopes (Jacobson and Holmden, 2008). Modeling tentatively suggests that dolomite recrystallization has a fractionation factor of 0‰ ($\alpha = 1.0000$) and that Mg-for-Na ion-exchange could have a fractionation factor of −0.60‰ ($\alpha = 0.9994$). However, additional laboratory experiments and field studies are required to test these hypotheses. Overall, we conclude that δ^{26}Mg values conservatively trace the cycling of Mg in carbonate-rich groundwater systems.

Acknowledgements

We thank F.-Z. Teng and an anonymous reviewer for constructive comments. This work was supported by NSF EAR-0617585 awarded to A. D. Jacobson. The mass spectrometry laboratory at UIUC is supported by NSF EAR-0732481.

References

Al-aasm, I.S., 2000. Chemical and isotopic constraints for recrystallization of sedimentary dolomites from the western Canada sedimentary basin. Aquat. Geochem. 6, 227–248.
Back, W., et al., 1983. Process and rate of dedolomitization: mass transfer and ^{14}C dating in a regional carbonate aquifer. Geol. Soc. Am. Bull. 94, 1415–1429.
Berner, R.A., Lasaga, A.C., Garrels, R.M., 1983. The carbonate-silicate geochemical cycle and its effect on atmospheric carbon dioxide over the past 100 million years. Am. J. Sci. 283 (7), 641–683.
Black, J.R., Yin, Q.-z., Casey, W.H., 2006. An experimental study of magnesium-isotope fraction in chlorophyll-a photosynthesis. Geochim. Cosmochim. Acta 70, 4072–4079.
Blankennagel, R.K., Howells, L.W., Miller, W.R., Hansen, C.V., 1979. Preliminary Data for Madison Limestone Test Well 3, NW 1/4, SE 1/4, Sec. 35, T. 2N., R. 27E. USGS Open File Report, Yellowstone Country, Montana, pp. 79–745. 186 pp.
Bolou-Bi, E.B., Vigier, N., Brenot, A., Poszwa, A., 2009. Magnesium isotope compositions of natural reference materials. Geostand. Geoanal. Res. 33 (1), 95–109.
Bolou-Bi, E.B., Poszwa, A., Leyval, C., Vigier, N., 2010. Experimental determination of magnesium-isotope fractionation during higher plant growth. Geochim. Cosmochim. Acta 74, 2523–2537.
Brenot, A., Cloquet, C., Vigier, N., Carignan, J., France-Lanord, C., 2008. Magnesium isotope systematics of the lithologically varied Moselle river basin, France. Geochim. Cosmochim. Acta 72 (20), 5070–5089.
Buhl, D., Immenhauser, A., Smeulders, G., Kabiri, L., Richter, D.K., 2007. Time series delta Mg-26 analysis in speleothem calcite: kinetic versus equilibrium fractionation, comparison with other proxies and implications for palaeoclimate research. Chem. Geol. 244 (3–4), 715–729.
Busby, J.F., Plummer, L.N., Lee, R.W., Hanshaw, B.B., 1991. Geochemical Evolution of Water in the Madison Aquifer in Parts of Montana. USGS Professional Paper, South Dakota and Wyoming, p. 89. 273-F.
de Villiers, S., Dickson, J.A.D., Ellam, R.M., 2005. The composition of the continental river weathering flux deduced from seawater Mg isotopes. Chem. Geol. 216 (1–2), 133–142.
Downey, J.S., 1984. Geohydrology of the Madison and Associated Aquifers in Parts of Montana. USGS Professional Paper, North Dakota, South Dakota, and Wyoming, p. 47. 1273-G.
Galy, A., Belshaw, N.S., Halicz, L., O Nions, R.K., 2001. High-precision measurement of magnesium isotopes by multiple-collector inductively coupled plasma mass spectrometry. Int. J. Mass Spectrom. 208, 89–98.
Galy, A., Bar-Matthews, M., Halicz, L., O'Nions, R.K., 2002. Mg isotopic composition of carbonate: insight from speleothem formation. Earth Planet. Sci. Lett. 201, 105–115.
Galy, A., Yoffe, O., Janney, P., Williams, R., Cloquet, C., Alard, O., Halicz, L., Wadhwa, M., Hutcheon, I., Ramon, E., Carignan, J., 2003. Magnesium isotope heterogeneity of the isotopic standard SRM980 and new reference materials for magnesium-isotope ratio measurements. J. Anal. At. Spectrom. 18, 1352–1356.
Hardie, L.A., 1996. Secular variation in seawater chemistry: an explanation for the coupled secular variation in the mineralogies of marine limestones and potash evaporites over the past 600 my. Geology 24 (3), 279–283.
Huang, F., Glessner, J., Ianno, A., Lundstrom, C., Zhang, Z., 2009. Magnesium isotopic composition of igneous rock standards measured by MC-ICP-MS. Chem. Geol. 268, 15–23.

Jacobson, A.D., Holmden, C., 2008. δ^{44}Ca evolution in a carbonate aquifer and its bearing on the equilibrium isotope fractionation factor for calcite. Earth Planet. Sci. Lett. 270, 349–353.

Jacobson, A.D., Wasserburg, G.J., 2005. Anhydrite and the Sr isotope evolution of groundwater in a carbonate aquifer. Chem. Geol. 214, 331–350.

Johnson, T.M., DePaolo, D.J., 1994. Interpretation of isotopic data in groundwater–rock systems: model development and application to Sr isotope data from Yucca Mountain. Water Resour. Res. 30, 1571–1587.

Johnson, T.M., DePaolo, D.J., 1997. Rapid exchange effects on isotope ratios in groundwater systems 1. Development of a transport-dissolution-exchange model. Water Resour. Res. 33, 187–195.

Kim, D.W., Jeon, B.K., Lee, N.S., Kim, C.S., Ryu, H.I., 2002. Magnesium isotope separation by ion exchange using hydrous manganese(IV) oxide. Talanta 57 (4), 701–705.

Long, A.J., Putnam, L.D., 2002. Flow-system analysis of the Madison and Minnelusa aquifers in the Rapid City area, South Dakota — conceptual model. Water Resour. Invest. Rep. U.S. Geol. Surv. 02–4185: 100 pp.

Miller, E.K., Blum, J.D., Friedland, A.J., 1993. Determination of soil exchangeable-cation loss and weathering rates using Sr isotopes. Nature 362 (6419), 438–441.

Naus, C.A., Driscoll, D.G., Carter, J.M., 2001. Geochemistry of the Madison and Minnelusa aquifers in the Black Hills area, South Dakota. Water Resour. Invest. Rep. U.S. Geol. Surv. 01–4129: 118 pp.

Negrel, P., Allegre, C.J., Dupre, B., Lewin, E., 1993. Erosion sources determined by inversion of major and trace element ratios and strontium isotopic ratios in river water: the Congo Basin case. Earth Planet. Sci. Lett. 120 (1–2), 59–76.

Plummer, L.N., Back, W., 1980. The mass balance approach: application to interpreting the chemical evolution of hydrologic systems. Am. J. Sci. 280, 130–142.

Plummer, L.N., Busby, J.F., Lee, R.W., Hanshaw, B.B., 1990. Geochemical modeling of the Madison Aquifer in parts of Montana, Wyoming, and South Dakota. Water Resour. Res. 26, 1981–2014.

Pogge von Strandmann, P., et al., 2008. The influence of weathering processes on riverine magnesium isotopes in a basaltic terrain. Earth Planet. Sci. Lett. 276, 187–197.

Richter, F.M., DePaolo, D.J., 1987. Numerical models for diagenesis and the neogene Sr isotopic evolution of seawater from DSDP site 590B. Earth Planet. Sci. Lett. 83 (1–4), 27–38.

Smith, T.M., Dorobek, S.L., 1993. Alteration of early-formed dolomite during shallow to deep burial: Mississippian Mission Canyon Formation, central to southwestern Montana. Geol. Soc. Am. Bull. 105, 1389–1399.

Thayer, P.A., 1983. Relationship of Porosity and Permeability to Petrology of the Madison Limestone in Rock Cores from Three Test Wells in Montana and Wyoming. USGS Professional Paper. 1273-C: 29 pp.

Tipper, E.T., Galy, A., Bickle, M.J., 2006. Riverine evidence for a fractionated reservoir of Ca and Mg on the continents: implications for the oceanic Ca cycle. Earth Planet. Sci. Lett. 247, 267–279.

Tipper, E.T., Galy, A., Bickle, M.J., 2008a. Calcium and magnesium isotope systematics in rivers draining the Himalaya–Tibetan-Plateau region: lithological or fractionation control? Geochim. Cosmochim. Acta 72, 1057–1075.

Tipper, E.T., Louvat, P., Capmas, F., Galy, A., Gaillardet, J., 2008b. Accuracy of stable Mg and Ca isotope data obtained by MC-ICP-MS using the standard addition method. Chem. Geol. 257, 65–75.

Wombacher, F., Eisenhauer, A., Heuser, A., Weyer, S., 2009. Separation of Mg, Ca and Fe from geological reference materials for stable isotope ratio analyses by MC-ICP-MS and double-spike TIMS. J. Anal. At. Spectrom. 24 (5), 627–636.

Young, E.D., Galy, A., 2004. The isotope geochemistry and cosmochemistry of magnesium. In: Johnson, C.M., Beard, B.L., Albarede, F. (Eds.), Geochemistry of Non-Traditional Stable Isotopes. Reviews in Mineralogy and Geochemistry, 55. Mineralogical Society of America, Washington D.C, pp. 197–230.